Organic & Biomolecular Chemistry

Cite this: *Org. Biomol. Chem.*, 2011, **9**, 2771

www.rsc.org/obc

PAPER

Phenazinolins A–E: novel diphenazines from a tin mine tailings-derived *Streptomyces* species†

Zhang-Gui Ding,[a] Ming-Gang Li,[a] Jie Ren,[b] Jiang-Yuan Zhao,[a] Rong Huang,[a] Qing-Zhong Wang,[a] Xiao-Long Cui,[a] Hua-Jie Zhu*[b] and Meng-Liang Wen*[a]

Received 8th January 2011, Accepted 17th January 2011
DOI: 10.1039/c1ob05044c

Phenazinolins A–E (**1–5**), which possess a carbon skeleton unique to diphenazines (the azabicyclo[3.3.1]nonadienol moiety in **1–3** and the oxabicyclo[3.3.1]nonadienol moiety in **4** and **5**), were isolated from tin mine tailings-derived *Streptomyces diastaticus* YIM DT26, with **1–3** exhibited appreciable cytotoxicity and antibiotic effects.

Introduction

Since the first discovery of the blue phenazine derivative pyocyanin by Fordos in the 1850s,[1] more than 100 phenazine pigments from various bacterial species, mainly from strains of *Pseudomonas* and *Streptomyces*, have received increasing attention because they have a biological significance beyond that of simple secondary metabolites.[2] The redox activity of phenazines enables them to function as electron shuttles and to reduce molecular oxygen to toxic reactive oxygen species, which is a possible basis for the antibiotic activity toward competitive bacterial and fungal pathogens in soil ecosystems or for the important virulence factors in infectious human diseases.[3] However, recent studies have demonstrated that phenazines also play unexpected roles in the physiology of the bacteria that generate them, such as controlling gene expression and biofilm formation,[4a] acting as a quorum sensing signal,[4b,4c] maintaining intracellular redox homeostasis,[4d] participating in iron acquisition in microbial communities,[4e,4f] and reoxidation of accumulating NADH to sustain glycolysis under aerobic conditions.[4g] Thus, the discovery of new phenazine derivatives would be useful to further elucidate the importance of these microbial metabolites.

In the course of our continuing studies,[5] *Streptomyces diastaticus* strain YIM DT26 was isolated from a soil sample collected from the Datun tin mine tailings area (103° 18′ 12″ E, 23° 18′ 48′ N), Yunnan, P.R. China.[6] The HPTLC and HPLC-DAD analysis of the ethyl acetate extract of *Streptomyces diastaticus* YIM DT26 showed the presence of new phenazine pigments. Silica gel flash chromatography, Sephadex LH-20 chromatography, and RP-HPLC of the crude extract led to the isolation of five novel diphenazines, phenazinolins A–E (**1–5**) (Scheme 1), along with the known compounds phenazine and phenazine-1-carboxylic acid (PCA). Herein, we report the complete structural assignment, with the absolute stereochemistry, and the biological activity of this new class of diphenazines, represented by phenazinolins A–E (**1–5**), isolated from a tin mine tailings-derived *Streptomyces*.

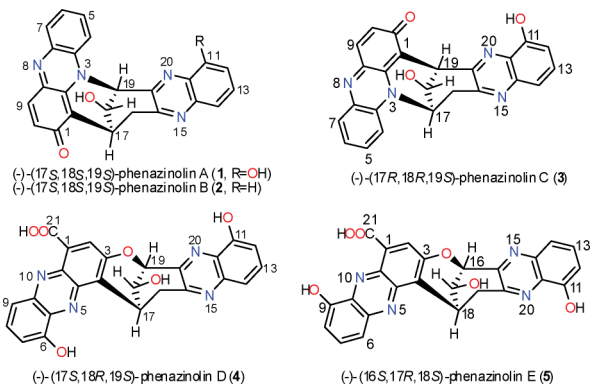

Scheme 1 Structures of phenazines isolated from *Streptomyces diastaticus* YIM DT26.

Results and discussion

The molecular formula of phenazinolin A (**1**), $C_{24}H_{16}N_4O_3$, was derived from the HRESIMS of the protonated molecular ion $[M + H]^+$ (*m/z*: found 409.1292, calcd 409.1295) and was in accord with the ^1H and ^{13}C NMR spectroscopic data. Accordingly, nineteen unsaturation indices were calculated for **1**. While the UV (MeOH) spectrum showed absorbance at λ_{max} 261 nm, the IR spectrum in KBr clearly suggested the presence of an iminoquinone based on an intense sharp band at 1600 cm^{-1} and showed the characteristic bands of a hydroxyl group at 3424 cm^{-1}.

[a]*Key Laboratory for Microbial Resources, Key Laboratory of Medicinal Chemistry for Natural Resources, Ministry of Education, Yunnan Institute of Microbiology, Yunnan University, Kunming 650091, PR China. E-mail: mlwen@ynu.edu.cn; Fax: +86 871 503 2170*

[b]*State Key Laboratory of Phytochemistry and Plant Resources in West China, Kunming Institute of Botany, Chinese Academy of Sciences, Kunming 650204, PR China. E-mail: hjzhu@mail.kib.ac.cn*

† Electronic supplementary information (ESI) available: Electronic Supplementary Information (ESI) available: Characterization data, 1D and 2D NMR, MS, and IR spectra for **1–5**, and a taxonomic description of the *Streptomyces diastaticus* YIM DT26. See DOI: 10.1039/c1ob05044c

Table 1 ^{1}H- (500 MHz) and ^{13}C-NMR (125 MHz) spectroscopic data (ppm) of phenazinolins A (**1**) and B (**2**) in DMSO-d_6[a]

	Phenazinolin A (**1**)		Phenazinolin B (**2**)	
Position	δ_C	δ_H (mult, J in Hz)	δ_C	δ_H (mult, J in Hz)
1	180.1 s		180.1 s	
2	109.4 s		109.4 s	
2a	131.7 s[b]		131.6 s	
3a	130.3 s		130.3 s	
4	116.4 d	8.88 (d, 8.6)	115.6 d	8.68 (d, 8.5)
5	132.7 d	7.87 (dd, 7.5, 8.6)[d]	132.4 d	7.92 (m)[f]
6	124.1 d	7.47 (t, 7.5)	124.0 d	7.49 (t, 7.9)
7	130.5 d	7.88 (d, 7.5)[d]	130.5 d[e]	7.91 (d, 7.9)[f]
7a	135.1 s		135.1 s	
8a	146.4 s[c]		146.4 s	
9	133.0 d	7.54 (d, 9.8)	133.0 d	7.55 (d, 9.8)
10	135.3 d	7.00 (d, 9.8)	135.3 d	7.00 (d, 9.8)
11	153.1 s		128.1 d	7.95 (d, 8.0)[f]
11-OH		10.06 (s)		
12	111.5 d	7.04 (d, 7.6)	130.6 d[e]	7.78 (m)
13	131.3 d	7.58 (t, 10.1)	129.5 d	7.72 (t, 8.6)
14	117.9 d	7.35 (d, 8.3)	128.5 d	7.93 (d, 8.6)[f]
14a	142.0 s		140.3 s	
15a	152.7 s		152.6 s	
16	33.7 t	3.59 (dd, 17.7, 5.5) 3.15 (dd, 17.7, 0.6)	33.4 t	3.65 (dd, 17.7, 5.0) 3.18 (dd, 17.7, 0.5)
17	30.2 d	3.70 (m)	30.3 d	3.70 (t, 5.0)
18	62.8 d	4.62 (dd, 4.0, 3.1)	62.7 d	4.63 (m)
18-OH		6.15 (br s)		6.11 (d, 2.4)
19	56.9 d	6.23 (dd, 4.0, 2.8)	56.6 d	6.34 (m)
19a	146.4 s[c]		148.9 s	
20a	131.6 s[b]		141.1 s	

[a] Assigned by COSY, HSQC, HMBC, and ROESY experiments. The multiplicity was measured in the DEPT experiment. [b] These two signals were interchangeable in terms of their assignments. [c] These two signals were interchangeable in terms of their assignments. [d] The signals of H-5 and H-7 in **1** overlapped. [e] These two signals were interchangeable in terms of their assignments. [f] The signals of H-5 and H-7, H-11 and H-14 in **2** overlapped.

The ^{13}C NMR spectra of **1** in DMSO-d_6 revealed the presence of one unsaturated ketone (δ_C 180.1, C-1), 10 olefinic/aromatic quaternary carbons, nine olefinic/aromatic methine carbons, two heteroatom-bearing methines [δ_C 62.8 (C-18) and δ_C 56.9 (C-19)], one methine, and one methylene group (Table 1). One carbonyl, 19 olefinic/aromatic carbons, and three sp^2-hybridized nitrogens accounted for a total of 12 unsaturation indices, with the remainder of the atoms being extrapolated into the seven rings of the molecule. Therefore, the remaining one nitrogen must be sp^3-hybridized for compatibility with the calculation of the unsaturation indices of **1**. Fourteen protons of the elemental composition $C_{24}H_{16}N_4O_3$ of **1** could be assigned unambiguously to their corresponding carbons in the HSQC spectrum (Fig. S4†). The remaining two protons were identified as hydrogen atoms of hydroxyl groups because the ^{1}H NMR signals at δ_H 10.06 (11-OH) and δ_H 6.15 (18-OH) immediately disappeared after addition of D_2O (20 μL) to the sample in DMSO-d_6. Analysis of the COSY and HMQC-TOCSY spectra of **1** revealed the presence of four discrete ^{1}H–^{1}H spin systems: H-4/H-5/H-6/H-7, H-9/H-10, H-12/H-13/H-14, and H_2-16/H-17/H-18/18-OH/H-19. Extensive analysis of the ^{1}H–^{13}C and ^{1}H–^{15}N HMBC spectra of **1** resulted in the determination of two main structural fragments: 1,10-disubstituted phenazin-2-one (**1a**) and 7,9-disubstituted tetrahydrophenazine-1,8-diol (**1b**) (Fig. 1). The positions of N-3, N-8, and N-15 were assigned unambiguously from the ^{1}H–^{15}N HMBC correlations of H-4 with N-3, H-7/H-9 with N-8, and H-14/H_2-16 with the N-15, respectively. **1a** and **1b** were linked through C-17/C-2 and C-19/N-3 from the HMBC correlations of H-17 with C-1/C-2/C-2a, H_2-16 with C-2, and H-19 with C-2a/C-3a, as well as the strong NOE correlation between H-19 and H-4. Combination of fragments **1a** and **1b** through the linkages of C-17/C-2 and C-19/N-3 resulted in an unique and very rigid azabicyclo[3.3.1]nonadienol ring system (Fig. 1).

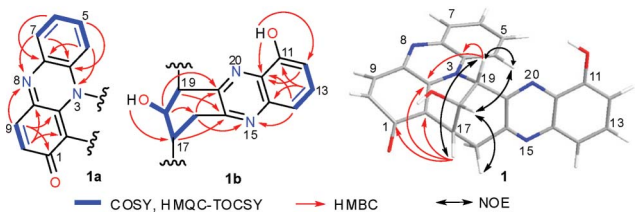

Fig. 1 Selected COSY, HMQC-TOCSY, HMBC, and ROESY correlations of **1a**, **1b**, and **1**.

The relative configuration of **1** was determined by analysis of its ^{1}H-NMR chemical shifts and 2D-ROESY correlations. In the ^{1}H-NMR spectrum of **1**, H-19 (δ_H 6.23, dd, 4.0, 2.8 Hz) was deshielded relative to H-17 (δ_H 3.70, m), indicating that H-19 should be equatorially orientated, causing the anisotropic deshielding effects of the two aromatic rings adjacent to C-19. In the ROESY plot (Fig. S9†), the signal of H-19 showed a strong correlation with that of H-4 also confirming H-19 to be equatorially oriented. NOE between H-17 and H-19 revealed an equatorial position for H-17, which led to an assignment of a *cis* configuration for the tetrahydropyridinol/cyclohexenol ring junction of **1** and an up situation of the ring for the bridged methine carbon C-18 (Fig. 1). The assignment of H-18 (δ_H 4.62, dd, 4.0, 3.1 Hz) in the axial position with respect to the cyclohexenol ring was derived from the small vicinal coupling constant between H-18 and H-19 ($^{3}J_{ax,eq}$ = 4.0 Hz), and NOE of H-18 with H-16$_{ax}$ (δ_H 3.15, dd, 17.7, 0.6 Hz). Thus, 18-OH should be in an equatorial position with respect to the cyclohexenol ring. This relative configuration was further confirmed by comparing the experimental ^{13}C NMR chemical shifts with the computed data using Gaussian03 package. All the errors were less than 5.0 (Fig. 2).

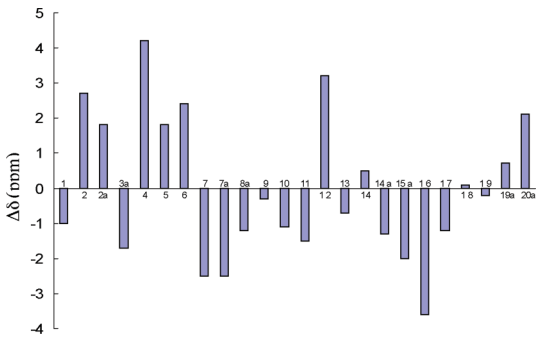

Fig. 2 The errors between the experimental ^{13}C NMR and the computed data for **1**.

Further computation of optical rotation (OR) values for **1** was performed using reported[7] and our previously used DFT

methods.[8] The ORs computed for **1** were +331° and +339° at the B3LYP/6-311++G(2d,p) level using B3LYP/6-31G(d)-optimized geometry and B3LYP/6-31+G(d,p)-optimized conformers, respectively. The recorded OR of **1** was −378°. Its absolute value (−378°) is very close to the computed data (from +331° to +339°) however, the OR signs are contrary. The proposed structure of **1** (Fig. 1) must be the enantiomer of the real geometry (Scheme 1). Accordingly, the absolute configurations of the three stereogenic centers in **1** are 17*S*, 18*S*, and 19*S*.

Structures of phenazinolins B–E (**2–5**) were elucidated by analogy to that of **1**. In the following section, we describe the elucidation of only the variable structural features. The molecular weight of phenazinolin B (**2**) was 16 amu lower $[M + H]^+$ (*m/z*: 393.1346) than that of **1** by HR-ESIMS. A molecular formula of $C_{24}H_{16}N_4O_2$ for **2** suggests that it is a deoxy analogue of **1**. Consistent with this deoxy structure, in the ^{13}C NMR spectra of **2** one oxygenated aromatic quaternary carbon signal (δ_C 153.1, C-11) in **1** was replaced by a signal for an aromatic methine carbon (δ_C 128.1, C-11) (Table 1). COSY and HMBC data of **2** (Fig. S17, S18†) revealed that **2** is the 11-deoxy analogue of **1**.

Phenazinolin C (**3**) has the same molecular formula as that of **1**, and its ^1H and ^{13}C NMR data were very similar to those of **1** (Table 2). The 2D NMR data demonstrated that the two identical structural fragments **1a** and **1b** were found in **3**; however, the linkage between **1a** and **1b** in **3** obviously differed from that in **1**. **1a** and **1b** were unambiguously linked through C-19/C-2 and C-17/N-3 on the basis of HMBC correlations of H-19 with C-1/C-2/C-2a, H-17 with C-2a/C-3a, and H_2-16 with N-3 (Fig. 3). Strong NOE correlation between H-17 and H-4 observed in the ROESY spectrum of **3** (Fig. S31†) supported the characterization of these linkages. The assignments of H-17, 18-OH, and H-19 to equatorial positions, and that of H-18 to an axial position with respect to the cyclohexenol ring, for **3** (Table S5, S6†) were the same as those for **1**.

The positive HRESIMS of phenazinolins D (**4**) and E (**5**) showed pseudomolecular ions at *m/z* 469.1135 and 469.1142, respectively, corresponding to their protonated molecular ions $[M + H]^+$ (*m/z*: calcd 469.1142). After inspection of their ^1H and ^{13}C NMR data (Table 3), the same formula, $C_{25}H_{16}N_4O_6$, was assigned to **4** and **5**. While structural fragment **1b** was also found in **4**, another fragment, 3,4-disubstituted 6-hydroxyphenazine-1-carboxylic acid (**4a**) (Fig. 4), was identified from 2D NMR spectral analysis. The linkage between **4a** and **1b** in **4** was very similar to the linkage between **1a** and **1b** in **1**, *i.e.*, the combination of **4a** and **1b** through the linkages of C-17/C-4 and C-19-O/C-3 formed an unique and very rigid oxabicyclo[3.3.1]nonadienol moiety in **4**. These linkages were supported by the HMBC correlations of H-17 with C-3/C-4, H_2-16 with C-4, and H-19 with C-3, as well as NOE correlations between H-18/H-19 and H-2 (Fig. 4). Regarding the relative stereochemistry of C-17, C-18, and C-19 in **4**, H-17, 18-OH, and H-19 were assigned to equatorial positions and H-18 to an axial position with respect to the dihydropyranol ring based on the following facts: (1) H-19 (δ_H 5.59, dd, 3.3, 1.8 Hz) was deshielded relative to H-17 (δ_H 4.83, m), (2) NOEs of H-19 with H-2 and H-17, (3) a small vicinal coupling constant between H-18 and H-19 ($^3J_{ax,eq}$ = 3.3 Hz). The structural assignment of **5** as the isomer of **4** was achieved by following a method similar to that described above (Fig. 4). The relative and absolute configurations of the three stereogenic centers in **2–5** were assigned by analysis of the ROESY spectra and comparison of ORs between recorded and computational values (Tables 4, S3–S11; Fig. S19, S31, S43, and S55†).

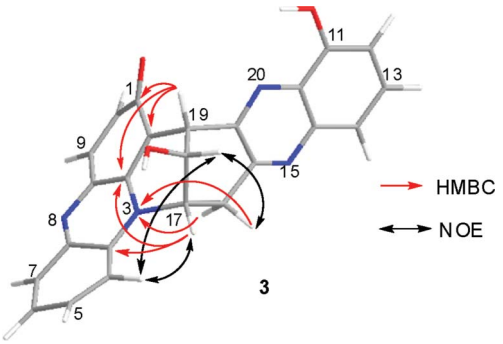

Fig. 3 Key HMBC and ROESY correlations of **3**.

Table 2 ^1H- (500 MHz) and ^{13}C-NMR (125 MHz) spectroscopic data (ppm) of phenazinolin C (**3**) in DMSO-d_6[a]

Position	δ_C	δ_H (mult, *J* in Hz)	Position	δ_C	δ_H (mult, *J* in Hz)
1	178.9 s		12	111.4 d	7.03 (d, 7.6)
2	106.4 s		13	129.9 d	7.49 (m)[b]
2a	132.3 s		14	117.7 d	7.27 (d, 8.4)
3a	130.5 s		14a	141.2 s	
4	114.2 d	8.02 (d, 8.8)	15a	150.6 s	
5	133.2 d	7.85 (m)	16	34.6 t	3.93 (dd, 19.2, 5.9)
6	124.3 d	7.52 (m)[b]			3.46 (dd)[c]
7	131.0 d	7.98 (d, 8.0)	17	52.5 d	5.40 m
7a	135.6 s		18	62.8 d	4.60 (dd, 4.4, 3.3)
8a	146.7 s		18-OH		6.18 (d 3.3)
9	132.7 d	7.54 (m)[b]	19	39.7 d	4.96 (dd, 4.4, 2.3)
10	135.5 d	6.94 (d, 9.6)	19a	151.4 s	
11	153.2 s		20a	131.8 s	
11-OH		10.34 (s)			

[a] Assigned by COSY, HSQC, ROESY, and HMBC experiments. The multiplicity was measured in the DEPT experiment. [b] The signals of H-6, H-9, and H-13 overlapped. [c] The signal was obscured by a signal due to water. After addition of D_2O in DMSO-d_6, δ_H 3.40 (d, 19.2).

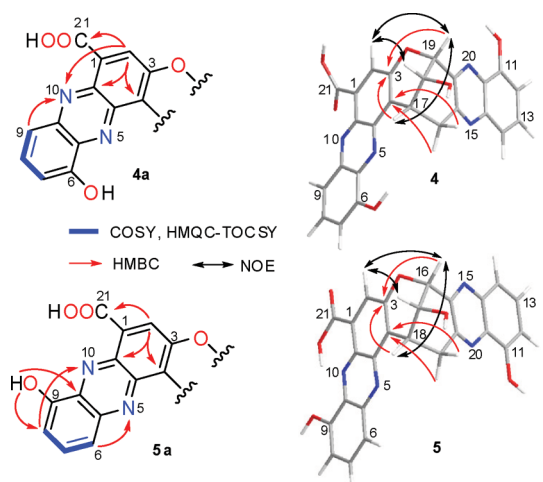

Fig. 4 Key COSY, HMQC-TOCSY, HMBC, and ROESY correlations of **4a**, **4**, **5a**, and **5**.

Table 3 ^{1}H- (500 MHz) and ^{13}C-NMR (125 MHz) spectroscopic data (ppm) of phenazinolins D (**4**) and E (**5**) in DMSO-d_6[a]

	Phenazinolin D (**4**)			Phenazinolin E (**5**)	
Position	δ_C	δ_H (mult, *J* in Hz)	Position	δ_C	δ_H (mult, *J* in Hz)
1	127.5 s		1	127.1 s	
2	127.8 d	7.92 (s)	2	127.9 d	7.90 (s)
3	151.1 s		3	151.0 s	
4	122.3 s		4	122.4 s	
4a	140.0 s		4a	140.0 s	
5a	135.2 s		5a	142.7 s	
6	153.3 s		6	117.8 d[f]	7.28 (d, 7.9)[h]
6-OH		10.68 (s)	7	131.4 d	7.57 (t, 7.9)
7	111.6 d[b]	7.29 (d, 8.0)[d]	8	111.6 d[g]	7.08 (d, 7.3)
8	132.5 d	7.80 (t, 8.0)	9	153.6 s	
9	118.0 d[c]	7.67 (d, 8.8)	9-OH		10.48 (s)
9a	139.3 s		9a	132.7 s	
10a	137.0 s		10a	136.9 s	
11	153.7 s		11	153.2 s	
11-OH		10.54 (s)	11-OH		10.62 (s)
12	111.6 d[b]	7.08 (d, 7.3)	12	111.6 d[g]	7.27 (d, 7.3)[h]
13	131.5 d	7.58 (t, 8.0)	13	132.5 d	7.77 (t, 8.6)
14	117.9 d[c]	7.27 (d, 7.3)[d]	14	117.8 d[f]	7.62 (d, 8.6)
14a	142.8 s		14a	139.1 s	
15a	152.9 s		15a	152.8 s	
16	34.6 t	3.86 (dd, 17.7, 5.1)	16	76.0 d	5.60 (dd, 3.4, 2.1)
		3.43 (dd)[e]	17	62.6 d	4.78 (m)
17	30.9 d	4.83 (m)	17-OH		6.16 (d, 2.4)
18	62.7 d	4.77 (m)	18	30.9 d	4.82 (m)
18-OH		6.19 (d, 2.9)	19	34.5 t	3.86 (dd, 17.4, 5.2)
19	76.1 d	5.59 (dd, 3.3, 1.8)			3.44 (dd)[e]
19a	146.4 s		19a	146.4 s	
20a	132.7 s		20a	135.1 s	
21	165.3 s		21	165.1 s	
21-OH		14.75 (br s)	21-OH		14.71 (br s)

[a] Assigned by COSY, HSQC, HMBC, and ROESY experiments. The multiplicity was measured in the DEPT experiment. [b] These two signals were interchangeable in terms of their assignments. [c] These two signals were interchangeable in terms of their assignments. [d] The signals of H-7 and H-14 in **1** overlapped. [e] The signal was obscured by a signal due to water. After addition of D_2O in DMSO-d_6, δ_H 3.14 (d, 17.5) in **4** and δ_H 3.22 (d, 17.4) in **5**. [f] These two signals were interchangeable in terms of their assignments. [g] These two signals were interchangeable in terms of their assignments. [h] The signals of H-6 and H-2 in **5** overlapped.

Table 4 Experimental, computed optical rotation (OR), and absolute configurations of C-17, C-18, and C-19 of phenazinolins A–E (**1–5**)

	Optical rotation (°)		
Compound	Experimental	Computed	Absolute configurations of C-17, C-18, and C-19
1	−378	+331 (low)[a] +339 (hi)[b]	17*S*, 18*S*, 19*S*
2	−259	+226 (low)[a] +216 (hi)[b]	17*S*, 18*S*, 19*S*
3	−1288	+1091 (low)[a] +1010 (hi)[b]	17*R*, 18*R*, 19*S*
4	−1559	+1314 (low)[a] +1314 (hi)[b]	17*S*, 18*R*, 19*S*
5	−1155	+969 (low)[a] +971 (hi)[b]	17*S*, 18*R*, 19*S*

[a] B3LYP/6-31G(d)-optimized geometries were used in OR computations. [b] B3LYP/6-31+G(d,p)-optimized geometries were used in OR computations.

The striking violet color of phenazinolins A–C (**1–3**), orange–red color of phenazinolin D (**4**), and dark-brown color of phenazinolin E (**5**) (Fig. 5) indicate that they have different chromophoric systems compared with that of the yellow–orange colored phenazine and PCA.[2c] While **1–3** possess

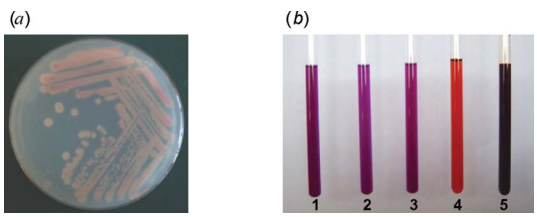

Fig. 5 (*a*) Streak plate of *Streptomyces diastaticus* YIM DT26. **1–5** turns the agar violet. (*b*) Methanol solutions of **1–5**.

1,10-disubstituted phenazin-2-one chromophores and a unique azabicyclo[3.3.1]nonadienol ring, **4**/**5** possess similar counterparts, *i.e.*, 3,4-disubstituted 6/9-hydroxyphenazine-1-carboxylic acids and an oxabicyclo[3.3.1]nonadienol ring. This is the first time these novel structural features have been observed among natural products. Interestingly, the linkage between **1a** and **1b** in **1** differed from that in **3**, and the position of hydroxyl group substitution differed between **4** and **5** (C-6 and C-9 positions, respectively). Compounds **1** and **3**, and **4** and **5**, likely share common biosynthetic precursors but have different homo/hetero-cyclization pathways.

Streptomyces-derived metabolites possessing structures similar to those of **1–5** include endophenazine B (**6**)[9] and esmeraldin B (**7**)[10] (Fig. 6). Both **1–3** and **6** possess the phenazin-2-one

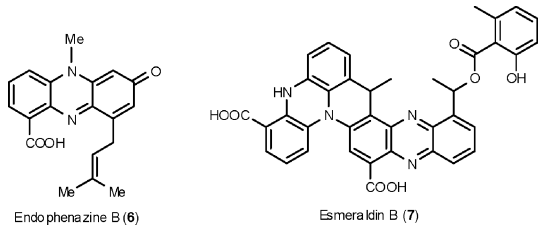

Fig. 6 Related metabolites from *Streptomyces*.

chromophoric system and exhibit a striking violet color; however, **1–3** are dimeric and **6** is monomeric. Furthermore, **1–5** have a more fused cyclic character than known diphenazines, such as phenazostatins A–D[11] and diphenazithionin.[12] While **1–5** possess the fundamental components of the phenazine class of bacterial pigments, the occurrence of the azabicyclo[3.3.1]nonadienol (in **1–3**) and oxabicyclo[3.3.1]nonadienol (in **4** and **5**) ring systems is intriguing and unprecedented. Although it has been confirmed that PCA is the biosynthetic precursor of **7**,[13] little is known about the assembly of **7** from shikimic acid pathway intermediates. The unique structural features of **1–5** may serve to elucidate the diphenazine biosynthetic pathway in *Streptomyces diastaticus* YIM DT26.

In our general bioactivity profiling program, **1–3** showed appreciable cytotoxicity and antibiotic effects, while **4** and **5** were devoid of activity. **1–3** exhibited *in vitro* cytotoxicity against P388, GLC, H460, and XWLC human cancer cell lines with IC_{50} values in the range of 14–40 μM. The MIC values of **1–3** for *Bacillus subtilis*, *Staphylococcus aureus*, *Aspergillus niger*, and *Botrytis cinerea* were in the range of 12–27 μM. Further evaluation of **1–3** in cancer-relevant bioassays and investigations of the physiological roles of **1–5** in the source organism *Streptomyces diastaticus* YIM DT26 are currently in progress.

Conclusions

In summary, a new class of diphenazines, represented by phenazinolins A–E (**1–5**), have been isolated from tin mine tailings-derived *Streptomyces diastaticus* YIM DT26, together with the known compounds phenazine and phenazine-1-carboxylic acid. The unique azabicyclo[3.3.1]nonadienol (in **1–3**) and oxabicyclo[3.3.1]nonadienol (in **4** and **5**) ring systems are intriguing and unprecedented among natural products. Their complete structural assignments with the absolute stereochemistry were characterized by spectroscopic data and calculation of optical rotation using DFT methods. **1–3** exhibited appreciable cytotoxicity and antibiotic effects.

Experimental

Strain and cultivation

Streptomyces sp. (YIM DT26) was isolated from a soil sample collected in the Datun tin mine tailings area (103°18′12″ E, 23°18′48″ N), Yunnan province, Southwest China. The soil in this area is contaminated with high contents of metals (including 1.4×10^5 mg kg^{-1} iron, 2.9×10^3 mg kg^{-1} tin, 1.8×10^3 mg kg^{-1} arsenic, 1.2×10^3 mg kg^{-1} copper, and 4.4×10^2 mg kg^{-1} lead). The strain, initially identified as a member of the genus *Streptomyces* on the basis of the morphological characteristics, was assigned as a strain of the species *Streptomyces diastaticus* by analysis of 16S rDNA sequence data (Genebank deposit no. GU289930, Fig. S1†). A voucher specimen is deposited at the Yunnan Institute of Microbiology, Yunnan University with the code YIM DT26. Strain YIM DT26 was cultured in 500 mL Erlenmeyer flasks (600 × 150 mL) in a soybean–mannitol medium (soybean flour 20 g L^{-1}, mannitol 20 g L^{-1}, pH 7.8 prior to sterilization) at 28 °C on a rotary shaker at 220 rpm for 5 d.

Extraction, isolation and purification

The completed fermentation broth (80 L) was separated into filtrate and pelleted bacterial cells by centrifugation. The culture filtrate was absorbed onto the Amberlite XAD-16 resin. After washing with deionized water, the organic material was obtained through elution with methanol. The eluate was concentrated to a slurry (5 L) *in vacuo*. The slurry material was extracted with ethyl acetate to yield 40 g of a dry crude extract, which was further chromatographed successively on: (1) silica gel (chloroform–methanol gradient), (2) Sephadex LH-20 (methanol), and by (3) semi-preparative HPLC (Waters SunFire C18 10 μm, 10 × 250 mm i.d., methanol–water gradient, 10 mL min^{-1}) to afford phenazinolins A (**1**, 18.2 mg), B (**2**, 2.5 mg), C (**3**, 10.5 mg), D (**4**, 16.8 mg), and E (**5**, 21.1 mg), along with the known compounds, phenazine (840 mg) and phenazine-1-carboxylic acid (384 mg).

Phenazinolin A (1). Violet solid. $[\alpha]_D^{20} = -378$ cm^3 g^{-1} dm^{-1} (c = 0.00004 g cm^{-3} in MeOH). UV (MeOH), λ_{max} (log ε) = 235.1 (4.9), 261.0 (5.0), 291.8 (4.9), 365.5 (4.4). IR (KBr) ν_{max} = 3424, 2918, 2854, 1626, 1600, 1528, 1511, 1468 cm^{-1}. m.p. >300 °C. 2D NMR data are summarized in Table S1.† HR-ESIMS: $C_{24}H_{16}N_4O_3$. $[M + H]^+$ m/z: calcd.: 409.1295, found: 409.1292. $[M + Na]^+$ m/z: calcd.: 431.1115, found: 431.1105. $[2M + Na]^+$ m/z: calcd.: 839.2337, found: 839.2349. $[M - H]^-$ m/z: calcd.: 407.1150, found: 407.1158. $[M + Cl]^-$ m/z: calcd.: 443.0916, found: 443.0932.

Phenazinolin B (2). Violet solid. $[\alpha]_D^{20} = -259$ cm^3 g^{-1} dm^{-1} (c = 0.00001 g cm^{-3} in MeOH). UV (MeOH), λ_{max} (log ε) = 236.3 (4.7), 294.2 (4.5), 365.5 (4.1). IR (KBr) ν_{max} = 3426, 2920, 2852, 1626, 1600, 1528, 1512, 1468 cm^{-1}. m.p. >300 °C. 2D NMR data are summarized in Table S3.† HR-ESIMS: $C_{24}H_{16}N_4O_2$. $[M + H]^+$ m/z: calcd.: 393.1346, found: 393.1346. $[M + Na]^+$ m/z: calcd.: 415.1166, found: 415.1182. $[2M + Na]^+$ m/z: calcd.: 807.2439, found: 807.2426. $[M - H]^-$ m/z: calcd.: 391.1201, found: 391.1206. $[M + Cl]^-$ m/z: calcd.: 427.0967, found: 427.0985. $[2M - H]^-$ m/z: calcd.: 783.2474, found: 783.2498.

Phenazinolin C (3). Violet solid. $[\alpha]_D^{20} = -1288$ cm^3 g^{-1} dm^{-1} (c = 0.00004 g cm^{-3} in MeOH). UV (MeOH), λ_{max} (log ε) = 235.1 (3.9), 259.9 (4.3), 295.4 (4.3), 362.3 (3.5). IR (KBr) ν_{max} = 3432, 2923, 2854, 1627, 1601, 1530, 1472 cm^{-1}. m.p. >300 °C. 2D NMR data are summarized in Table S5.† HR-ESIMS: $C_{24}H_{16}N_4O_3$. $[M + H]^+$ m/z: calcd.: 409.1295, found: 409.1294. $[M + Na]^+$ m/z: calcd.: 431.1115, found: 431.1113. $[2M + Na]^+$ m/z: calcd.: 839.2337, found: 839.2317. $[M - H]^-$ m/z: calcd.: 407.1150, found: 407.1154. $[M + Cl]^-$ m/z: calcd.: 443.0916, found: 443.0943.

Phenazinolin D (4). Orange–red solid. $[\alpha]_D^{20} = -1559$ cm^3 g^{-1} dm^{-1} (c = 0.00098 g cm^{-3} in MeOH). UV (MeOH), λ_{max} (log ε) = 271.7 (4.4), 382.3 (3.9). IR (KBr) ν_{max} = 3428, 3067, 2921, 2852,

1713, 1626, 1607, 1574, 1548, 1525, 1478, 1457, 1424 cm^{-1}. m.p. >300 °C. 2D NMR data are summarized in Table S7.† HR-ESIMS: $C_{25}H_{16}N_4O_6$. $[M + H]^+$ *m/z*: calcd.: 469.1143, found: 469.1135. $[M + Na]^+$ *m/z*: calcd.: 491.0962, found: 491.0919. $[M - H]^-$ *m/z*: calcd.: 467.0997, found: 467.1003. $[2M - H]^-$ *m/z*: calcd.: 935.2067, found: 935.2091.

Phenazinolin E (5). Brown solid. $[\alpha]_D^{20} = -1155$ cm^3 g^{-1} dm^{-1} (c = 0.00038 g cm^{-3} in MeOH). UV (MeOH), λ_{max} (log ε) = 271.7 (4.5), 382.3 (4.0). IR (KBr) ν_{max} = 3420, 3065, 2920, 2853, 1712, 1624, 1607, 1573, 1548, 1525, 1478, 1456, 1423 cm^{-1}. m.p. >300 °C. 2D NMR data are summarized in Table S9.† HR-ESIMS: $C_{25}H_{16}N_4O_6$. $[M + H]^+$ *m/z*: calcd.: 469.1143, found: 469.1142. $[M + Na]^+$ *m/z*: calcd.: 491.0962, found: 491.0963. $[M - H]^-$ *m/z*: calcd.: 467.0997, found: 467.0997. $[2M - H]^-$ *m/z*: calcd.: 935.2067, found: 935.2061.

Computational method

All compound conformations were searched using a Hyperchem soft package using Amber force field. The stable conformations were then optimized at the B3LYP/6-31G(d) and B3LYP/6-31+G(d,p) level in the gas phase, respectively. OR computations were performed at the B3LYP/6-311++G(2d,p) level using the B3LYP/6-31G(d) and B3LYP/6-31+G(d,p)-optimized geometries, respectively. Boltzmann statistics were used in all molecular OR computations. The computed ORs for all compounds are summarized in Table S11.† The computed ^{13}C NMR shielding obtained at the B3LYP/6-311++G(2d,p) level were then converted into chemical shifts and corrected using our previously reported methods.[14] The errors between the experimental ^{13}C NMR and the computed data for phenazinolins A–E (**1–5**) were listed in Tables S2, S4, S6, S8, and S10, respectively.†

Acknowledgements

This work was supported by the Yunnan University (21131033), NSFC (31060011, 30770235, 30873141), and 973 Program (2009CB522300).

Notes and references

1 M. J. Fordos, *Recl. Trav. Soc. d'Emul. Sci. Pharm.*, 1859, **3**, 30.
2 (*a*) J. B. Laursen and J. Nielsen, *Chem. Rev.*, 2004, **104**, 1663–1685; (*b*) D. V. Mavrodi, W. Blankenfeldt and L. S. Thomashow, *Annu. Rev. Phytopathol.*, 2006, **44**, 417–445; (*c*) A. Price-Whelan, L. E. Dietrich and D. K. Newman, *Nat. Chem. Biol.*, 2006, **2**, 71–78; (*d*) M. Mentel, E. G. Ahuja, D. V. Mavrodi, R. Breinbauer, L. S. Thomashow and W. Blankenfeldt, *ChemBioChem*, 2009, **10**, 2295–2304.
3 (*a*) T. F. C. Chin-A-Woeng, G. V. Bloemberg and B. J. J. Lugtenberg, *New Phytol.*, 2003, **157**, 503–523; (*b*) G. W. Lau, D. J. Hassett, H. Ran and F. Kong, *Trends Mol. Med.*, 2004, **10**, 599–606.
4 (*a*) L. E. Dietrich, T. K. Teal, A. Price-Whelan and D. K. Newman, *Science*, 2008, **321**, 1203–1206; (*b*) M. Whiteley, K. M. Lee and E. P. Greenberg, *Proc. Natl. Acad. Sci. U. S. A.*, 1999, **96**, 13904–13909; (*c*) L. E. Dietrich, A. Price-Whelan, A. Petersen, M. Whiteley and D. K. Newman, *Mol. Microbiol.*, 2006, **61**, 1308–1321; (*d*) M. E. Hernandez and D. K. Newman, *Cell. Mol. Life Sci.*, 2001, **58**, 1562–1571; (*e*) M. E. Hernandez, A. Kappler and D. K. Newman, *Appl. Environ. Microbiol.*, 2004, **70**, 921–928; (*f*) E. Banin, M. L. Vasil and E. P. Greenberg, *Proc. Natl. Acad. Sci. U. S. A.*, 2005, **102**, 11076–11081; (*g*) A. Price-Whelan, L. E. Dietrich and D. K. Newman, *J. Bacteriol.*, 2007, **189**, 6372–6381.
5 Z. G. Ding, M. G. Li, J. Y. Zhao, J. Ren, R. Huang, M. J. Xie, X. L. Cui, H. J. Zhu and M. L. Wen, *Chem.–Eur. J.*, 2010, **16**, 3902–3905.
6 Strain YIM DT26's partial 16S rRNA sequence (Genbank #GU289930) is 99.57% identical to *Streptomyces diastaticus* NRRLB1773^T.
7 (*a*) F. J. Devlin, P. J. Stephens, C. Oesterle, K. B. Wiberg, J. R. Cheeseman and M. J. Frisch, *J. Org. Chem.*, 2002, **67**, 8090–8096; (*b*) P. Wipf and S. R. Spencer, *J. Am. Chem. Soc.*, 2005, **127**, 225–235; (*c*) G. Zuber, M. R. Goldsmith, T. D. Hopkins, D. N. Beratan and P. Wipf, *Org. Lett.*, 2005, **7**, 5269–5272; (*d*) E. Giorgio, M. Roje, K. Tanaka, Z. Hamersak, V. Sunic, K. Nakanishi, C. Rosini and N. Berova, *J. Org. Chem.*, 2005, **70**, 6557–6563; (*e*) X. W. Yang, Y. Ding, X. C. Li, D. Ferreira, Y. H. Shen, S. M. Li, N. Wang and W. D. Zhang, *Chem. Commun.*, 2009, 3771–3773.
8 (*a*) H. J. Zhu, *Modern Organic Stereochemistry*, Science Press, Beijing, 2009, pp. 1–52, pp. 211–282; (*b*) J. Ren, J. X. Jiang, L. B. Li, T. G. Liao, R. R. Tian, X. L. Chen, S. P. Jiang, C. U. Pittman Jr. and H. J. Zhu, *Eur. J. Org. Chem.*, 2009, 3987–3991.
9 P. Krastel, A. Zeeck, K. Gebhardt, H. P. Fiedler and J. Rheinheimer, *J. Antibiot*, 2002, **55**, 801–806.
10 W. Keller-Schierlein, A. Geiger, H. Zähner and M. Brandl, *Helv. Chim. Acta*, 1988, **71**, 2058–2070.
11 (*a*) B. S. Yun, I. J. Ryoo, W. G. Kim, J. P. Kim, H. Koshino, H. Seto and I. D. Yoo, *Tetrahedron Lett.*, 1996, **37**, 8529–8530; (*b*) W. G. Kim, I. J. Ryoo, B. S. Yun, K. Shin-ya, H. Seto and I. D. Yoo, *J. Antibiot.*, 1999, **52**, 758–761; (*c*) R. P. Maskey, I. Kock, E. Helmke and H. Laatsch, *Z. Naturforsch.*, 2002, **57b**, 823–829.
12 Y. Hosoya, H. Adachi, H. Nakamura, Y. Nishimura, H. Naganawa, Y. Okami and T. Takeuchi, *Tetrahedron Lett.*, 1996, **37**, 9227–9228.
13 (*a*) C. Van't Land, U. Mocek and H. G. Floss, *J. Org. Chem.*, 1993, **58**, 6576–6582; (*b*) M. McDonald, B. Wilkinson, C. Van't Land, U. Mocek, S. Lee and H. G. Floss, *J. Am. Chem. Soc.*, 2001, **123**, 5619–5624.
14 J. X. Pu, S. X. Huang, J. Ren, W. L. Xiao, L. M. Li, R. T. Li, L. B. Li, T. G. Liao, L. G. Luo, H. J. Zhu and H. D. Sun, *J. Nat. Prod.*, 2007, **70**, 1706–1711.

